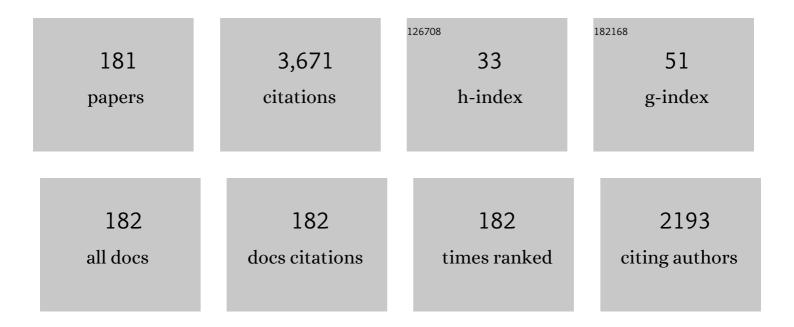
List of Publications by Year in descending order

Source: https://exaly.com/author-pdf/1499099/publications.pdf Version: 2024-02-01



YONGUANG HUANG

#	Article	IF	CITATIONS
1	Exceptionally high glass-forming ability of an FeCoCrMoCBY alloy. Applied Physics Letters, 2005, 86, 151907.	1.5	325
2	Zr–Cu–Ni–Al bulk metallic glasses with superhigh glass-forming ability. Acta Materialia, 2009, 57, 1290-1299.	3.8	118
3	Engineering Microdomains of Oxides in Highâ€Entropy Alloy Electrodes toward Efficient Oxygen Evolution. Advanced Materials, 2021, 33, e2101845.	11.1	90
4	A new Ti–Zr–Hf–Cu–Ni–Si–Sn bulk amorphous alloy with high glass-forming ability. Journal of Alloys and Compounds, 2007, 427, 171-175.	2.8	82
5	Indentation creep of an Fe-based bulk metallic glass. Intermetallics, 2009, 17, 190-194.	1.8	78
6	Controllable additive manufacturing of gradient bulk metallic glass composite with high strength and tensile ductility. Acta Materialia, 2021, 206, 116632.	3.8	78
7	Superplasticity and superplastic forming ability of a Zr–Ti–Ni–Cu–Be bulk metallic glass in the supercooled liquid region. Journal of Non-Crystalline Solids, 2005, 351, 209-217.	1.5	75
8	Enhanced strength and plasticity of a Ti-based metallic glass at cryogenic temperatures. Materials Science & Engineering A: Structural Materials: Properties, Microstructure and Processing, 2008, 498, 203-207.	2.6	68
9	Synthesis of Fe–Cr–Mo–C–B amorphous coating with high corrosion resistance. Materials Letters, 2012, 89, 229-232.	1.3	67
10	Microstructure and mechanical properties of Fe CoCrNiMn high-entropy alloys. Journal of Materials Science and Technology, 2019, 35, 2331-2335.	5.6	66
11	Stochastic deformation and shear transformation zones of the glassy matrix in CuZr-based metallic-glass composites. International Journal of Plasticity, 2020, 125, 52-62.	4.1	64
12	Columnar to equiaxed transition in additively manufactured CoCrFeMnNi high entropy alloy. Materials and Design, 2021, 197, 109262.	3.3	62
13	Strengthening CrFeCoNiMn0.75Cu0.25 high entropy alloy via laser shock peening. International Journal of Plasticity, 2022, 154, 103296.	4.1	60
14	High tensile plasticity and strength of a CuZr-based bulk metallic glass composite. Materials and Design, 2016, 90, 145-150.	3.3	59
15	Low-modulus biomedical Ti–30Nb–5Ta–3Zr additively manufactured by Selective Laser Melting and its biocompatibility. Materials Science and Engineering C, 2019, 97, 275-284.	3.8	58
16	Combined current-modulation annealing induced enhancement of giant magnetoimpedance effect of Co-rich amorphous microwires. Journal of Applied Physics, 2014, 115, 17A326.	1.1	54
17	A CuZr-based bulk metallic glass composite with excellent mechanical properties by optimizing microstructure. Journal of Non-Crystalline Solids, 2018, 483, 94-98.	1.5	54
18	The onset of plasticity of a Zr-based bulk metallic glass. International Journal of Plasticity, 2014, 60, 87-100.	4.1	52

#	Article	IF	CITATIONS
19	The effect of cooling rate on the wear performance of a ZrCuAlAg bulk metallic glass. Materials & Design, 2014, 58, 284-289.	5.1	49
20	Mechanical performance of metallic glasses during nanoscratch tests. Intermetallics, 2010, 18, 1056-1061.	1.8	47
21	Fabrication and Characterization of Melt-Extracted Co-Based Amorphous Wires. Metallurgical and Materials Transactions A: Physical Metallurgy and Materials Science, 2011, 42, 1103-1108.	1.1	46
22	Magnetocaloric effect of Ni-Fe-Mn-Sn microwires prepared by melt-extraction technique. Materials and Design, 2017, 114, 1-9.	3.3	45
23	Indentation size effect of hardness of metallic glasses. Materials & Design, 2010, 31, 1563-1566.	5.1	43
24	Nanoindentation study of Ti-based metallic glasses. Journal of Alloys and Compounds, 2009, 479, 121-128.	2.8	42
25	Elucidating how correlated operation of shear transformation zones leads to shear localization and fracture in metallic glasses: Tensile tests on Cu Zr based metallic-glass microwires, molecular dynamics simulations, and modelling. International Journal of Plasticity, 2019, 119, 1-20.	4.1	42
26	Enhanced magnetocaloric and mechanical properties of melt-extracted Gd55Al25Co20 micro-fibers. Journal of Alloys and Compounds, 2014, 603, 167-171.	2.8	41
27	The relationship between thermo-mechanical history, microstructure and mechanical properties in additively manufactured CoCrFeMnNi high entropy alloy. Journal of Materials Science and Technology, 2021, 77, 187-195.	5.6	41
28	A new TiCuHfSi bulk metallic glass with potential for biomedical applications. Materials & Design, 2014, 54, 251-255.	5.1	39
29	Tuning the mechanical performance of a Ti-based bulk metallic glass by pre-deformation. Intermetallics, 2010, 18, 2044-2050.	1.8	38
30	Structure and mechanical property modification of a Ti-based metallic glass by ion irradiation. Scripta Materialia, 2015, 103, 41-44.	2.6	37
31	In vitro and in vivo biocompatibility of an Ag-bearing Zr-based bulk metallic glass for potential medical use. Journal of Non-Crystalline Solids, 2015, 419, 82-91.	1.5	36
32	Enhanced tensile plasticity of a CuZr-based bulk metallic glass composite induced by ion irradiation. Journal of Materials Science and Technology, 2019, 35, 2221-2226.	5.6	36
33	Critical cooling rate and thermal stability for a Ti–Zr–Ni–Cu–Be metallic glass. Journal of Alloys and Compounds, 2009, 477, 920-924.	2.8	35
34	Enhanced magnetocaloric properties of melt-extracted GdAlCo metallic glass microwires. Journal of Magnetism and Magnetic Materials, 2014, 372, 23-26.	1.0	32
35	Laser additive manufacturing of structural-graded bulk metallic glass. Journal of Alloys and Compounds, 2018, 766, 506-510.	2.8	32
36	Electrochemical and XPS studies of a Nb-containing Ti-based glass-forming alloy system in H 2 SO 4 solution. Electrochemistry Communications, 2015, 60, 139-143.	2.3	31

#	Article	IF	CITATIONS
37	316L Stainless Steel Manufactured by Selective Laser Melting and Its Biocompatibility with or without Hydroxyapatite Coating. Metals, 2018, 8, 548.	1.0	31
38	Cryogenic mechanical behaviors of CrMnFeCoNi high-entropy alloy. Materials Science & Engineering A: Structural Materials: Properties, Microstructure and Processing, 2020, 789, 139579.	2.6	31
39	Magnetostructural coupling and magnetocaloric effect in Ni-Mn-Ga-Cu microwires. Applied Physics Letters, 2016, 108, .	1.5	30
40	Superplastic formability of a Zr–Ti–Ni–Cu–Be bulk metallic glass. Journal of Alloys and Compounds, 2006, 415, 198-203.	2.8	29
41	Bending behavior of as-cast and annealed ZrCuNiAl bulk metallic glass. Journal of Materials Science and Technology, 2017, 33, 1153-1158.	5.6	29
42	Nanocrystallization enabled tensile ductility of Co-based amorphous microwires. Scripta Materialia, 2012, 66, 1041-1044.	2.6	28
43	High temperature deformation behaviors of Ti40Zr25Ni3Cu12Be20 bulk metallic glass. Journal of Alloys and Compounds, 2010, 504, S82-S85.	2.8	26
44	Close correlation between transport properties and glass-forming ability of an FeCoCrMoCBY alloy system. Intermetallics, 2012, 30, 144-147.	1.8	25
45	Graded structure of laser direct manufacturing bulk metallic glass. Intermetallics, 2018, 103, 67-71.	1.8	25
46	The effects of annealing on the microstructure and the dynamic mechanical strength of a ZrCuNiAl bulk metallic glass. Intermetallics, 2013, 42, 192-197.	1.8	24
47	Design of Fe-containing GdTbCoAl high-entropy-metallic-glass composite microwires with tunable Curie temperatures and enhanced cooling efficiency. Materials and Design, 2021, 206, 109824.	3.3	24
48	Enhancing the magnetocaloric response of high-entropy metallic-glass by microstructural control. Science China Materials, 2022, 65, 1134-1142.	3.5	24
49	Shear punching of a Ti-based bulk metallic glass. Materials Science & Engineering A: Structural Materials: Properties, Microstructure and Processing, 2013, 561, 220-225.	2.6	23
50	Atomic structure evolution of high entropy metallic glass microwires at cryogenic temperature. Scripta Materialia, 2019, 163, 29-33.	2.6	23
51	Tunable Magnetocaloric Effect in Ni-Mn-Ga Microwires. Scientific Reports, 2018, 8, 16574.	1.6	22
52	Optimization of GMI properties by AC Joule annealing in meltâ€extracted Coâ€rich amorphous wires for sensor applications. Physica Status Solidi (A) Applications and Materials Science, 2014, 211, 1577-1582.	0.8	21
53	Influence of microstructure evolution on GMI properties and magnetic domains of melt-extracted Zr-doped amorphous wires with accumulated DC annealing. Journal of Alloys and Compounds, 2015, 644, 180-185.	2.8	21
54	Serration and shear avalanches in a ZrCu based bulk metallic glass composite in different loading methods. Journal of Materials Science and Technology, 2019, 35, 2079-2085.	5.6	21

YONGJIANG HUANG

#	Article	IF	CITATIONS
55	Temperature influence on sintering with concurrent crystallization behavior in Ti-based metallic glassy powders. Materials Science & Engineering A: Structural Materials: Properties, Microstructure and Processing, 2010, 527, 2662-2668.	2.6	20
56	Optimization of mechanical and giant magnetoâ€impedance (GMI) properties of meltâ€extracted Coâ€rich amorphous microwires. Physica Status Solidi (A) Applications and Materials Science, 2014, 211, 1668-1673.	0.8	20
57	Comparison of mechanical behaviors of several bulk metallic glasses for biomedical application. Journal of Non-Crystalline Solids, 2014, 406, 144-150.	1.5	20
58	Dilatancy of Shear Transformations in a Colloidal Glass. Physical Review Applied, 2018, 9, .	1.5	20
59	Table-like magnetocaloric behavior and enhanced cooling efficiency of a Bi-constituent Gd alloy wire-based composite. Journal of Alloys and Compounds, 2018, 764, 789-793.	2.8	20
60	Joining of Zr 51 Ti 5 Ni 10 Cu 25 Al 9 BMG to aluminum alloy by friction stir welding. Vacuum, 2015, 120, 47-49.	1.6	19
61	In situ study of the shear band features of a CuZr-based bulk metallic glass composite. Intermetallics, 2019, 112, 106523.	1.8	19
62	Enhanced ablation resistance of HfB2-HfC/SiBCN ceramics under an oxyacetylene torch environment. Corrosion Science, 2021, 187, 109509.	3.0	19
63	Enhanced tensile properties and wear resistance of additively manufactured CoCrFeMnNi high-entropy alloy at cryogenic temperature. Rare Metals, 2022, 41, 1210-1216.	3.6	19
64	Understanding the deformation mechanism of individual phases of a ZrTi-based bulk metallic glass matrix composite using <i>in situ</i> diffraction and imaging methods. Applied Physics Letters, 2014, 104, 031912.	1.5	18
65	The temperature dependent dynamic mechanical response of a ZrCuNiAl bulk metallic glass. Materials Science & Engineering A: Structural Materials: Properties, Microstructure and Processing, 2012, 551, 100-103.	2.6	17
66	Free volume and viscosity of Fe–Co–Cr–Mo–C–B–Y bulk metallic glasses and their correlation with glass-forming ability. Journal of Non-Crystalline Solids, 2012, 358, 1274-1277.	1.5	17
67	Effect of Co addition on the shear viscosity of Fe-based bulk metallic glasses. Journal of Non-Crystalline Solids, 2014, 403, 62-66.	1.5	17
68	Effect of ion irradiation in an Al90Fe2Ce8 metallic glass. Materials & Design, 2014, 62, 133-136.	5.1	17
69	Magnetocaloric effect of melt-extracted high-entropy Gd19Tb19Er18Fe19Al25 amorphous microwires. Journal of Magnetism and Magnetic Materials, 2020, 507, 166856.	1.0	17
70	A new strategy to overcome the strength-ductility trade off of high entropy alloy. Scripta Materialia, 2022, 214, 114678.	2.6	17
71	Microstructure and crystallization mechanism of Ti-based bulk metallic glass by electron beam welding. Journal of Manufacturing Processes, 2018, 32, 93-99.	2.8	16
72	Quantitatively determining the martensitic transformation in a CuZr-based bulk metallic glass composite. Journal of Alloys and Compounds, 2019, 782, 961-966.	2.8	16

#	Article	IF	CITATIONS
73	The electronic structure origin for ultrahigh glass-forming ability of the FeCoCrMoCBY alloy system. Journal of Applied Physics, 2011, 110, .	1.1	15
74	Single crystal titanate–zirconate nanoleaf: Synthesis, growth mechanism and enhanced photocatalytic hydrogen evolution properties. CrystEngComm, 2012, 14, 1874.	1.3	15
75	Specific heat capacities of Fe–Co–Cr–Mo–C–B–Y bulk metallic glasses and their correlation with glass-forming ability. Materials Letters, 2015, 143, 191-193.	1.3	15
76	Comparable magnetocaloric properties of melt-extracted Gd36Tb20Co20Al24 metallic glass microwires. Journal of Alloys and Compounds, 2020, 815, 150983.	2.8	14
77	Formation, thermal stability and mechanical properties of Ti42.5Zr7.5Cu40Ni5Sn5 bulk metallic glass. Science in China Series G: Physics, Mechanics and Astronomy, 2008, 51, 372-378.	0.2	13
78	Thermodynamic characteristics of Ti-based glass-forming alloys. Journal of Non-Crystalline Solids, 2009, 355, 986-990.	1.5	13
79	Enhanced Curie temperature and cooling efficiency in melt-extracted Gd50(Co69.25Fe4.25Si13B13.5)50 microwires. Journal of Alloys and Compounds, 2017, 708, 678-684.	2.8	13
80	Three-dimensional reconstruction of bifilm defects. Scripta Materialia, 2021, 191, 179-184.	2.6	13
81	Elucidating the transition of cryogenic deformation mechanism of CrMnFeCoNi high entropy alloy. Journal of Alloys and Compounds, 2021, 872, 159606.	2.8	13
82	Structural evolution of a CuZr-based bulk metallic glass composite during cryogenic treatment observed by in-situ high-energy X-ray diffraction. Journal of Alloys and Compounds, 2021, 871, 159570.	2.8	13
83	Tridimensional morphology and kinetics of etch pit on the {0001} plane of sapphire crystal. Journal of Solid State Chemistry, 2012, 192, 60-67.	1.4	12
84	Ductile Ti-based metallic glass spheres. Scripta Materialia, 2012, 67, 661-664.	2.6	12
85	Magnetocaloric effect and critical behavior in melt-extracted Gd <sub>60</sub> Co <sub>15</sub> Al <sub>25</sub> microwires. Physica Status Solidi (A) Applications and Materials Science, 2015, 212, 1905-1910.	0.8	12
86	Microstructure and thermal conductivity of hypereutectic Al-high Si produced by casting and spray deposition. Journal of Materials Research, 2016, 31, 2948-2955.	1.2	12
87	Effect of Double Oxide Film Defects on Mechanical Properties of As-Cast C95800 Alloy. Acta Metallurgica Sinica (English Letters), 2017, 30, 541-549.	1.5	12
88	Hierarchical microstructure of a titanium alloy fabricated by electron beam selective melting. Journal of Materials Science and Technology, 2020, 42, 1-9.	5.6	12
89	New DyHoCo medium entropy amorphous microwires of large magnetic entropy change. Journal of Alloys and Compounds, 2020, 837, 155431.	2.8	12
90	Overcoming the strength-ductility trade-off in an additively manufactured CoCrFeMnNi high entropy alloy via deep cryogenic treatment. Additive Manufacturing, 2022, 50, 102546.	1.7	12

#	Article	IF	CITATIONS
91	First-principle calculations for electronic structure and bonding properties in layered Na2Ti3O7. Open Physics, 2011, 9, .	0.8	11
92	Surface microstructural design to improve mechanical and giant magneto-impedance properties of melt-extracted CoFe-based amorphous wires. Materials and Design, 2021, 204, 109642.	3.3	11
93	Bending behavior of TiZrNiCuBe bulk metallic glass. Journal of Alloys and Compounds, 2012, 541, 359-364.	2.8	10
94	Brazing of Ti2AlNb based alloy with amorphous Ti-Cu-Zr-Ni filler. Journal Wuhan University of Technology, Materials Science Edition, 2015, 30, 617-621.	0.4	10
95	Composite electroplating to enhance the GMI output stability of melt-extracted wires. Materials and Design, 2016, 96, 251-256.	3.3	10
96	Strain-field evolution in a CuZr-based bulk metallic glass composite during tensile deformation. Materials Science & Engineering A: Structural Materials: Properties, Microstructure and Processing, 2017, 697, 233-237.	2.6	10
97	Understanding the structure-Poisson's ratio relation in bulk metallic glass. Journal of Materials Science, 2018, 53, 7891-7899.	1.7	10
98	In-mold oxidation behavior of Mg–4.32Y–2.83Nd–0.41Zr alloy. Journal of Materials Science, 2018, 53, 11091-11103.	1.7	10
99	Temperature-dependent deformation behavior of a CuZr-based bulk metallic glass composite. Journal of Alloys and Compounds, 2021, 858, 158368.	2.8	10
100	Tensile Strength Reliability Analysis of Cu48Zr48Al4 Amorphous Microwires. Metals, 2016, 6, 296.	1.0	9
101	Evolved gas analysis of PEP-SET sand by TG and FTIR. Journal of Analytical and Applied Pyrolysis, 2017, 127, 490-495.	2.6	9
102	Cryogenic-temperature-induced phase transformation in a CuZr-based bulk metallic glass composite under tensile stress. Materials Letters, 2020, 262, 127065.	1.3	9
103	Microstructure Evolution and Mechanical Properties of PM-Ti43Al9V0.3Y Alloy. Materials, 2020, 13, 198.	1.3	9
104	Cooling rate effect of nanomechanical response for a Ti-based bulk metallic glass. Journal of Non-Crystalline Solids, 2010, 356, 966-970.	1.5	8
105	Resistance spot welding of Ti40Zr25Ni3Cu12Be20 bulk metallic glass: experiments and finite element modeling. Rare Metals, 2017, 36, 123-128.	3.6	8
106	Mössbauer study of the ultrahigh glass-forming ability in FeCoCrMoCBY alloy system. Vacuum, 2017, 141, 173-175.	1.6	8
107	The Magnetocaloric Composite Designed by Multiâ€Cdâ€Alâ€Co Microwires with Close Performances. Physica Status Solidi (A) Applications and Materials Science, 2019, 216, 1900090.	0.8	8
108	Oxide bifilm defects in aluminum alloy castings. Materials Letters, 2021, 285, 129089.	1.3	8

#	Article	IF	CITATIONS
109	Precipitation behavior in a Nb-5W-2Mo-1Zr niobium alloy fabricated by electron beam selective melting. Materials Characterization, 2021, 174, 111019.	1.9	8
110	Magnetocaloric effect in Ni–Fe–Mn–Sn microwires with nano-sized γ precipitates. Applied Physics Letters, 2020, 116, .	1.5	8
111	Bonding Layer Microstructures and Mechanical Behavior of Sapphire/Sapphire Joints Diffusion-bonded using MgO-Al2O3-SiO2 Interlayer. International Journal of Applied Ceramic Technology, 2011, 8, 1183-1191.	1.1	7
112	Shape memory effects of Ni <sub>49.7</sub> Mn <sub>25.0</sub> Ga <sub>19.8</sub> Fe <sub>5.5</sub> microwires prepared by rapid solidification. Physica Status Solidi (A) Applications and Materials Science, 2014, 211, 2532-2536.	0.8	7
113	Martensite transformation and magnetic properties of Ni <sub>50</sub> Mn <sub>25</sub> Ga <sub>25–</sub> <i><sub>x</sub></i> Fe <i><sub>x</sub></i> ferromagnetic microwires for application in microdevices. Physica Status Solidi (A) Applications and Materials Science, 2015, 212, 855-861.	0.8	7
114	The effect of stress concentration on the bending behavior of a ZrCuNiAl bulk metallic glass. Journal of Non-Crystalline Solids, 2017, 469, 19-26.	1.5	7
115	Tensile Creep Characterization and Prediction of Zr-Based Metallic Glass at High Temperatures. Metals, 2018, 8, 457.	1.0	7
116	Cavity etching evolution on the A-plane of sapphire crystal in molten KOH etchant. Journal of Crystal Growth, 2020, 552, 125926.	0.7	7
117	Study on stochastic nature of plasticity of Cu/Zr metallic glass micropillars. Journal of Alloys and Compounds, 2020, 831, 154719.	2.8	7
118	Microstructure evolution and globularization mechanism of lamellar phases in Ti6.5Al2Zr1Mo1V produced by electron beam melting. Journal of Materials Research and Technology, 2021, 14, 1921-1933.	2.6	7
119	Atomic study on deformation behaviors of crystal-glass nanocomposite with a typical hierarchical structure. Computational Materials Science, 2022, 206, 111287.	1.4	7
120	Improvement of giant magneto impedance of Co-rich melt extraction wires by stress-current annealing. Rare Metals, 2011, 30, 327-331.	3.6	6
121	Theoretical analysis of the shape evolution of crystals grown by pulling. Crystal Research and Technology, 2011, 46, 1019-1026.	0.6	6
122	Process design for the shape control of crystals grown by Kyropoulos or SAPMAC method. Crystal Research and Technology, 2012, 47, 175-182.	0.6	6
123	Liquid-solid joining of bulk metallic glasses. Scientific Reports, 2016, 6, 30674.	1.6	6
124	The study of preparation process of spray formed 7075/Al–Si bimetallic gradient composite plate. Journal of Materials Research, 2017, 32, 3109-3116.	1.2	6
125	Fine tuning the microstructure and mechanical properties of a Zr-based bulk metallic glass using electropulsing treatment. Journal of Alloys and Compounds, 2019, 789, 704-711.	2.8	6
126	Biocompatibility of a micro-arc oxidized ZrCuAlAg bulk metallic glass. Journal of Materials Research and Technology, 2021, 13, 486-497.	2.6	6

#	Article	IF	CITATIONS
127	The Formation Mechanism of Porosity for Spray-deposited 7075 Alloy. Materials Research, 2015, 18, 89-94.	0.6	6
128	EFFECT OF <font>Ce</font> ON GRAPHITE NODULE COUNT AND SIZE DISTRIBUTION IN DUCTILE IRON. International Journal of Modern Physics B, 2009, 23, 1853-1860.	1.0	5
129	Calculating activation energy of amorphous phase with the Lambert W function. Journal of Thermal Analysis and Calorimetry, 2010, 100, 3-10.	2.0	5
130	Bulk amorphous Al85Ni10Ce5 composite fabricated by cold hydro-mechanical pressing of partially amorphous powders. Science Bulletin, 2011, 56, 3965-3971.	1.7	5
131	Haze in sapphire crystals grown by SAPMAC method. Crystal Research and Technology, 2011, 46, 669-675.	0.6	5
132	Effect of grain size on the microstructure and mechanical properties of Mg-4Y-3Nd-0.5Zr alloy. International Journal of Materials Research, 2014, 105, 607-609.	0.1	5
133	Long-term room-temperature aging treatment of a bulk metallic glass composite. Journal of Alloys and Compounds, 2020, 820, 153165.	2.8	5
134	Tensile deformation mechanism of a bulk metallic glass matrix composite using in situ neutron diffraction. Journal of Non-Crystalline Solids, 2020, 546, 120267.	1.5	5
135	Influence of Fe-doping amounts on magnetocaloric properties of Gd-based amorphous microfibers. Journal of Alloys and Compounds, 2020, 845, 156190.	2.8	5
136	Real-Time Terrain-Following of an Autonomous Quadrotor by Multi-Sensor Fusion and Control. Applied Sciences (Switzerland), 2021, 11, 1065.	1.3	5
137	In situ study on the bending strain field of a Zr-based bulk metallic glass with notch. Materials Characterization, 2021, 174, 111001.	1.9	5
138	Determining deformation behaviors in a CuZr-based bulk metallic glass composite. Journal of Non-Crystalline Solids, 2021, 561, 120768.	1.5	5
139	Creep behaviors of a Mg–Li based alloy at elevated temperatures. Materials Science & Engineering A: Structural Materials: Properties, Microstructure and Processing, 2021, 827, 142063.	2.6	5
140	MECHANICAL PROPERTY OF A NEW <font>Zr</font> -BASED BULK METALLIC GLASS WITH CERTAIN PLASTICITY AT LOW TEMPERATURE. International Journal of Modern Physics B, 2009, 23, 1331-1336.	1.0	4
141	Crystallization of a Ti-based Bulk Metallic Glass Induced by Electropulsing Treatment. Journal of Iron and Steel Research International, 2016, 23, 69-73.	1.4	4
142	Plasticity improvement of a Zr-based bulk metallic glass by micro-arc oxidation. Journal of Iron and Steel Research International, 2017, 24, 416-420.	1.4	4
143	Nanoscratching and mechanical behaviors of high-entropy alloys with different phase constituents. Journal of Iron and Steel Research International, 2019, 26, 1240-1248.	1.4	4
144	Temperature-induced atomic structural evolution in a liquid Ga-based alloy. Vacuum, 2019, 170, 108966.	1.6	4

YONGJIANG HUANG

#	Article	IF	CITATIONS
145	Etching Behaviors of Sapphire's C- Plane Cavity. Surface Science, 2021, 707, 121805.	0.8	4
146	Relative contributions of different substrates to soil N2O emission and their responses to N addition in a temperate forest. Science of the Total Environment, 2021, 767, 144126.	3.9	4
147	Shear punching of a Co20Cr20Fe20Ni20Mn15Cu5 high entropy alloy. Journal of Alloys and Compounds, 2021, 887, 161415.	2.8	4
148	Diverse microstructure of Ti6.5Al2Zr1Mo1V fabricated via electron beam selective melting. Materials Letters, 2021, 304, 130597.	1.3	4
149	Cooling-rate induced softening in a colloidal glass. Scientific Reports, 2017, 7, 16882.	1.6	3
150	Manufacture and characterization of HoErCo medium-entropy alloy microwires with excellent magnetic entropy change. Journal of Non-Crystalline Solids, 2021, 556, 120570.	1.5	3
151	Structure of oxide bifilms in nickel-aluminium bronze alloys. Applied Surface Science, 2021, 541, 148491.	3.1	3
152	Dislocation Etching Morphology on the A Plane of Sapphire Crystal. Crystal Research and Technology, 2021, 56, 2100022.	0.6	3
153	Thermal Expansion Behavior of Co-Spray Formed Al-20Si/7075 Bimetallic Gradient Alloy. Materials, 2021, 14, 4100.	1.3	3
154	A virtual velocity-based integrated navigation method for strapdown inertial navigation system and Doppler velocity logÂcoupled with unknown current. Review of Scientific Instruments, 2022, 93, .	0.6	3
155	Investigation of precipitation phases in as-cast wedge ingot of bulk amorphous Zr56.6Cu17.3Ni12.5Al9.6Ti4 alloy. Journal of Alloys and Compounds, 2009, 481, 531-538.	2.8	2
156	Influence of the Crystalline Phase on Strain-Rate Sensitivity of a Zr-Cu-Ni-Al Bulk Metallic Glass at Room Temperature. Metallurgical and Materials Transactions A: Physical Metallurgy and Materials Science, 2012, 43, 5202-5208.	1.1	2
157	Oxidation and Ignition Behaviors of Molten Mg-Nd-Zr Alloy in Resin-Sand Mold. Journal of Materials Engineering and Performance, 2019, 28, 5344-5351.	1.2	2
158	Magnetocaloric effect and microstructure of amorphous/nanocrystalline HoErFe melt-extracted microwires. Intermetallics, 2020, 127, 106974.	1.8	2
159	Shear transformation zone dependence of creep behaviors of amorphous phase in a CuZr-based bulk metallic glass composite. Science China Technological Sciences, 2020, 63, 1560-1565.	2.0	2
160	Hot Deformation Behavior and Microstructural Evolution of PM Ti43Al9V0.3Y with Fine Equiaxed Î <sup>3</sup> and B2 Grain Microstructure. Materials, 2020, 13, 896.	1.3	2
161	Tunable Linear Dependence of Giant Magnetoimpedance Response of Microwires Annealed under Fluid Oil for Sensor Applications. Physica Status Solidi (A) Applications and Materials Science, 2021, 218, 2100154.	0.8	2
162	Shrinked bifilms in Mg-Gd-Y-Zr alloy. Materials Letters, 2022, 306, 130906.	1.3	2

#	Article	IF	CITATIONS
163	Intermediate-Temperature Tensile Behavior of a Hot-Rolled Mg-Li-Al-Cd-Zn Alloy. Materials, 2022, 15, 1686.	1.3	2
164	Tensile Properties of Melt-Extracted and Annealed Ni/Fe-Based Amorphous Metallic Fibers. Metals, 2022, 12, 918.	1.0	2
165	Reverse Plasticity in Nanoindentation. Materials Research Society Symposia Proceedings, 2007, 1049, 1.	0.1	1
166	Quantitative process design of 1-D crystallization for pure melt. Metals and Materials International, 2010, 16, 725-730.	1.8	1
167	DIAMETER DEPENDENCE OF GIANT MAGNETO-IMPEDANCE EFFECT IN <font>Co</font> -BASED MELT EXTRACTED AMORPHOUS WIRES. , 2011, , .		Ο
168	The local structure nature for a Ti-based bulk metallic glass. Materials Science and Engineering B: Solid-State Materials for Advanced Technology, 2013, 178, 117-121.	1.7	0
169	Differences in crystallisation behaviours during cooling and post-heating processes of Ti based metallic powders. Powder Metallurgy, 2013, 56, 32-37.	0.9	Ο
170	Magnetocaloric effect and critical behavior in melt-extracted Gd <sub>60</sub> Co <sub>15</sub> Al <sub>25</sub> microwires (Phys. Status Solidi A 9â^•2015). Physica Status Solidi (A) Applications and Materials Science, 2015, 212, n/a-n/a.	0.8	0
171	Dataset on the microstructure Ni50Mn38Sb9Si3 alloy and compositions of Ni50Mn38Sb12â^'Si (x=2.5, 3) ferromagnetic shape memory alloys. Data in Brief, 2018, 19, 222-225.	0.5	Ο
172	The Application of Canned Deformation to a Hard-Deformed Spray-Deposited Al-Zn-Mg-Cu Alloy. Journal of Materials Engineering and Performance, 2019, 28, 3531-3538.	1.2	0
173	Visualizing flow-unit-mediated deformation in a simple glass. Scripta Materialia, 2019, 165, 154-158.	2.6	Ο
174	Dataset on comparable magnetocaloric properties of melt-extracted Gd36Tb20Co20Al24 metallic glass microwires. Data in Brief, 2020, 28, 104960.	0.5	0
175	Hot deformation behavior of A390 alloy produced by semi ontinuous cast. Material Design and Processing Communications, 2020, 2, e148.	0.5	Ο
176	Hot deformation and dynamic recrystallization behavior of a powder metallurgy Tiâ€45Alâ€6Nbâ€0.3W alloy. Material Design and Processing Communications, 2021, 3, e224.	0.5	0
177	Hot Deformation Behavior of a Co-Spray-Formed Al-Si/7075 Bimetallic Gradient Alloy. Metals, 2021, 11, 1266.	1.0	Ο
178	Preliminary study on deformation behaviors of spray droplet impacting on nonrigid deposited layer. Material Design and Processing Communications, 2021, 3, e263.	0.5	0
179	The Effect of Spray-Formed Al22Si Coating on Wear Resistance Performance. Materials Performance and Characterization, 0, , 20160117.	0.2	0
180	Atomization Characteristics of Droplet and Morphologies of Arc Sprayed Ni-Al Particles and Composition Coatings. Materials Research, 2019, 22, .	0.6	0

#	Article	IF	CITATIONS
181	Ion irradiation effect on mechanical properties and corrosion resistance of a Cu <sub>50</sub> Zr <sub>50</sub> metallic glass. Advanced Engineering Materials, 0, , .	1.6	0